PERGAMON

International Journal of Solids and Structures 38 (2001) 183–201

INTERNATIONAL JOURNAL OF SOLIDS and STRUCTURES

www.elsevier.com/locate/ijsolstr

Effective elastoplastic behavior of metal matrix composites containing randomly located aligned spheroidal inhomogeneities. Part I: micromechanics-based formulation

J.W. Ju [a,*], L.Z. Sun [b]

[a] *Department of Civil and Environmental Engineering, University of California, Los Angeles, 5731/5732 Boelter Hall, Los Angeles, CA 90095-1593, USA*

[b] *Department of Civil and Environmental Engineering, Center for Computer-Aided Design, The University of Iowa, Iowa City, IA 52242-1527, USA*

Received 5 August 1998

Abstract

Based on the framework of Ju and Chen (Ju, J.W., Chen, T.M., 1994. J. Engng. Mater. Tech. ASME 116, 310–318) and Ju and Tseng (Ju, J.W., Tseng, K.H., 1996. Int. J. Solids Struct. 33, 4267–4291; Ju, J.W., Tseng, K.H., 1997. J. Engng. ASCE 123, 260–266), we study the effective elastoplastic behavior of two-phase metal matrix composites (MMCs) containing randomly located yet unidirectionally aligned spheroidal inhomogeneities. Specifically, the particle phase is assumed to be linearly elastic and the matrix phase is elastoplastic. The ensemble-volume averaging procedure is employed to micromechanically derive the effective yield function of MMCs based on the *probabilistic* spatial distribution of aligned spheroidal particles and the particle-matrix influences. The transversely isotropic effective elasticity tensor is explicitly derived. Further, the associative plastic flow rule and the isotropic hardening law are postulated according to the continuum plasticity. As a result, we can characterize the overall elastoplastic stress–strain responses of aligned spheroid-reinforced MMCs under three-dimensional loading and unloading histories. The overall elastoplastic continuum tangent tensor of MMCs is also explicitly presented.

Keywords: Metal matrix composites; Mirco mechanics; Effective elastoplastic behavior

1. Introduction

The prediction and estimation of overall mechanical properties of random heterogeneous materials are of great interest to researchers and engineers in many science and engineering disciplines. The so-called ''effective'' properties of a heterogeneous composite can be obtained by some volume and ensemble averaging processes over a ''representative volume element'' (RVE) featuring a ''mesoscopic'' length scale, which is much larger than the characteristic length scale of microscopic particles (inhomogeneities or inclusions) but smaller than the characteristic length scale of a macroscopic specimen. Metal matrix composites (MMCs)

* Corresponding author. Tel.: +1-310-206-1751; fax: +1-310-267-2283.
E-mail address: juj@ucla.edu (J.W. Ju).

0020-7683/00/$ - see front matter
PII: S0020-7683(00)00023-8

are one class of multiphase materials, usually consisting of two phases (e.g., with ceramics as the reinforcement and metal as the matrix). With the advent of new processing techniques, the mechanical properties, which can be tailored with MMCs, such as the low density, high strength and high stiffness, have made MMCs attractive candidate materials for aerospace, automotive and many structural applications. In MMCs, reinforcements may be continuous in the form of long fibers or discontinuous in the form of particulates, short fibers or whiskers. Although continuous fiber-reinforced MMCs offer highly directional properties such as high specific stiffness along the fiber direction, discontinuously reinforced MMCs have attracted considerable attentions as they provide a number of advantages. For example, particle-reinforced MMCs (PRMMCs) are less expensive to produce and they can be shaped by standard metallurgical processes such as forging, rolling and extrusion, etc. Further, PRMMCs can exhibit nearly isotropic behavior (if randomly oriented). We refer to Taya and Arsenault (1989), Ibrahim et al. (1991), Suresh et al. (1993), Clyne and Withers (1993), and Arsenault et al. (1994) for a general review of PRMMCs.

A topic of practical importance regarding the applications of discontinuously reinforced MMCs is the prediction of their effective elastoplastic behavior from microstructural characteristics. These include the mechanical properties of constituent phases, volume fractions, spatial distributions, and micro-geometries (shapes, orientations and sizes) of inhomogeneities. For instance, Tandon and Weng (1988) employed the Mori-Tanaka method Mori and Tanakaa (1973) and the secant moduli method (cf. Berveiller and Zaoui, 1979) to predict the effective elastoplasticity of PRMMCs. Subsequently, Zhao and Weng (1990) considered the overall elastoplasticity of aligned spheroid reinforced MMCs. However, as pointed out by the authors themselves, the above approach is not reasonably acceptable under a high hydrostatic loading. Therefore, an improved method was proposed by Qiu and Weng (1992, 1993, 1995), using the *energy criterion* for the effective stress of the ductile matrix to estimate the strain potential and the overall stress–strain relations of a two-phase composite containing spherical or spheroidal inclusions.

A different strategy involves the so-called mathematical upper and lower bounds, and variational estimates. Along this line, Ponte Castaneda (1991, 1992, 1996) provided the estimates for isotropic particulate composites and fiber reinforced composites. In addition, Li (1992) and Li and Ponte Castaneda (1994) proposed the estimates for spheroidal PRMMCs. On the contrary, Suquet (1993) proposed a different mathematical bounding method, which is less general than the previous methods, but simpler for the cases considered therein.

Based on Budiansky et al. (1982) and Duva (1984), Lee and Mear (1991, 1992) considered the effects of inclusion shape on the strength of power-law composites. First, they solved a kernel problem for an *isolated* inclusion in an infinite block, and obtained constitutive relations for dilute inclusion concentrations. Subsequently, they employed a differential self-consistent scheme to extend their formulation to non-dilute concentrations. By contrast, motivated by the work of Gurson (1977), Zhu and Zbib (1995) employed a finite unit cell to account for the interaction effects of particles in MMCs with periodic microstructures. They provided an upper bound solution for the flow strength of MMCs.

In addition, it is popular to use the finite element analysis to investigate the mechanical behavior of PRMMCs. For instance, Christman et al. (1989a,b) and Tvergaard (1990) calculated the effective elastoplastic behavior of short-fiber reinforced MMCs by using the axisymmetric unit cell (periodic) model. Similarly, Levy and Papazian (1990) and Hom (1992) utilized a unit cell model together with the three-dimensional finite element analysis to determine the effective elastoplastic responses of short-fiber reinforced MMCs. Moreover, Bao et al. (1991) combined the finite element analysis with a theoretical investigation.

Emanating from the continuum (not micromechanical) approach, some researchers treat MMCs as single-phase anisotropic materials with different properties along different directions. Naturally, the behavior of the aligned short-fiber or continuous-fiber reinforced MMCs exhibit at least transverse isotropy. Important works along this line include, for example, the continuum model of Mulhern et al. (1967), the failure criteria of Hashin (1980), and the bimodal plasticity analysis of Dvorak and Bahei-El-Din (1987)

and Dvorak (1988) for fiber reinforced MMCs. Hansen et al. (1991) and Schmidt et al. (1993) also proposed a modified model of Hill (1948) to calculate the plastic behavior of transversely isotropic composites. Further, Voyiadjis and Thiagarajan (1995) proposed a new anisotropic pressure-dependent continuum yield surface model for directional fiber-reinforced MMCs.

More recently, Ju and Chen (1994a–c) and Ju and Tseng (1996, 1997) developed a new micromechanical framework to predict the effective elastic and elastoplastic behavior of spherical PRMMCs with *random* microstructures, under three-dimensional loading and unloading histories. They considered both the "noninteracting" (far-field interacting) and interacting formulations involving elastic *spherical* particles embedded in an elastoplastic metal matrix. Further extending their work, the present article aims to predict the overall elastoplastic stress–strain responses of randomly located, aligned *spheroid*-reinforced MMCs.

The rest of the article is organized as follows. In Section 2, following the very recent work of Ju and Sun (1999), local micromechanics is recapitulated to render an explicit expression for the "exterior-point Eshelby's tensor", which represents the strain/stress influence of an *ellipsoidal* inclusion upon a material point located within the *matrix* phase. Rigorous mathematical and geometric quantities are used to obtain the explicit expressions. Assuming a simple J_2-type plasticity for the matrix material, the ensemble-average procedure is utilized in Section 3 to derive the overall "current stress norm" of aligned spheroid-reinforced MMCs. Subsequently, the effective yield function is derived in Section 4. Further, the overall associative plastic flow rule and the isotropic hardening law are postulated. As a result, we arrive at a micromechanics-based elastoplastic constitutive formulation for aligned spheroid-reinforced MMCs under three-dimensional loading and unloading conditions. In a companion article (Sun and Ju, 2000), applications to the uniaxial, hydrostatic and axisymmetric elastoplastic stress–strain behavior will be considered in detail. Comparison among our model predictions, experimental data, finite element results, and mathematical bounds will also be presented in a companion article to illustrate the capability and performance of the proposed framework.

2. Local micromechanics of an ellipsoidal inhomogeneity embedded in an elastic medium

Let us start by considering a composite consisting of a linearly elastic isotropic matrix (phase 0) and unidirectionally aligned linearly elastic isotropic ellipsoidal inclusions (phase 1) with distinct material properties (Fig. 1(a)). It is assumed that the two phases are perfectly bonded at interfaces.

Upon loading, the total stress $\boldsymbol{\sigma}(\mathbf{x})$ at any local point $\mathbf{x}$ in the matrix is the sum of the far-field stress $\boldsymbol{\sigma}^0$ and the perturbed stress $\boldsymbol{\sigma}'(\mathbf{x})$ due to the presence of the inhomogeneities (Fig. 2). Specifically, we have

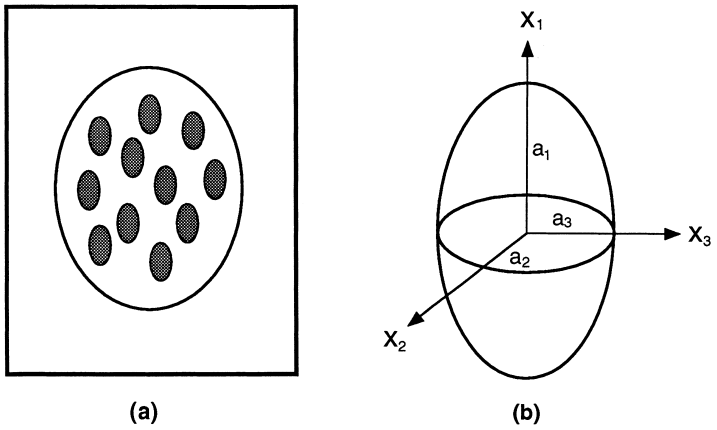

Fig. 1. (a) A composite containing randomly located, aligned ellipsoidal particles, and (b) Sketch of an ellipsoid.

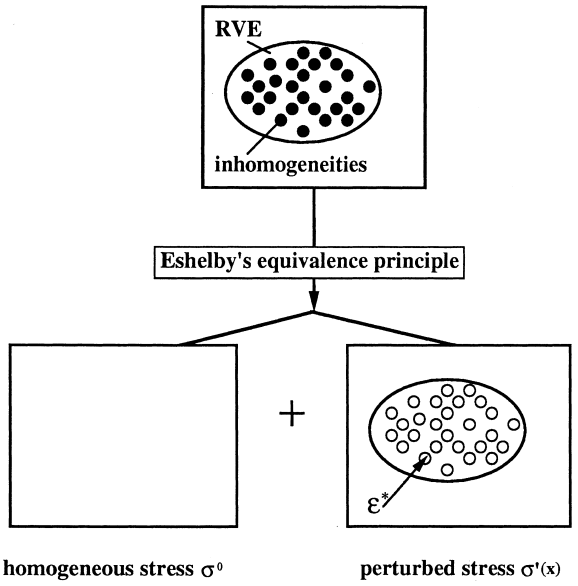

Fig. 2. Superposition of a homogeneous medium with the far-field stress $\boldsymbol{\sigma}^0$, and another homogeneous medium with the perturbed stress $\boldsymbol{\sigma}'(\mathbf{x})$.

$\boldsymbol{\sigma}^0 = \mathbf{C}_0 : \boldsymbol{\epsilon}^0$, and the stress perturbation due to one single inhomogeneity $\Omega_1(\mathbf{x}^{(1)})$ centered at $\mathbf{x}^{(1)}$ is derived as (cf. Ju and Chen, 1994a,b,c)

$$\boldsymbol{\sigma}'(\mathbf{x}|\mathbf{x}^{(1)}) = [\mathbf{C}_0 \cdot \bar{\mathbf{G}}(\mathbf{x} - \mathbf{x}^{(1)})] : \boldsymbol{\epsilon}^{*0}, \tag{1}$$

where $\mathbf{C}_0$ is the linear elasticity tensor of the matrix, the symbol ":" denotes the tensor contraction, and $\boldsymbol{\epsilon}^0$ is the uniform elastic strain field induced by the far-field loading. In addition, $\boldsymbol{\epsilon}^{*0}$ denotes the *noninteracting* solution of the (elastic) eigenstrain for the isolated inclusion problem (cf. Eshelby, 1957).

The so-called "exterior-point Eshelby's tensor" $\bar{\mathbf{G}}(\mathbf{x} - \mathbf{x}^{(1)})$ is defined as (cf. Ju and Sun, 1999)

$$\bar{\mathbf{G}}(\mathbf{x} - \mathbf{x}^{(1)}) = \int_{\Omega_1(\mathbf{x}^{(1)})} \mathbf{G}(\mathbf{x} - \mathbf{x}')\,\mathrm{d}\mathbf{x}' \tag{2}$$

for $\mathbf{x} \notin \Omega_1(\mathbf{x}^{(1)})$. In indicial notation, the components of the fourth-rank Green's function tensor $\mathbf{G}$ read (cf. Ju and Chen, 1994a)

$$\begin{aligned} G_{ijkl}(\mathbf{x} - \mathbf{x}') = \frac{1}{8\pi(1-\nu_0)\|\mathbf{x} - \mathbf{x}'\|^3} \big[&(1-2\nu_0)(\delta_{ik}\delta_{jl} + \delta_{il}\delta_{jk} - \delta_{ij}\delta_{kl}) + 3\nu_0(\delta_{ik}n_j n_l + \delta_{il}n_j n_k \\ &+ \delta_{jk}n_i n_l + \delta_{jl}n_i n_k) + 3\delta_{ij}n_k n_l + 3(1-2\nu_0)\delta_{kl}n_i n_j - 15 n_i n_j n_k n_l\big], \end{aligned} \tag{3}$$

where ν_0 is Poisson's ratio of the matrix material, and the outward unit vector is defined as $\mathbf{n} = (\mathbf{x} - \mathbf{x}')/\|\mathbf{x} - \mathbf{x}'\|$. The symbol $\|\cdot\|$ signifies the norm of a vector. We denote by V the statistical RVE, which is infinitely large compared to inclusions and without any prescribed displacement boundary conditions along the infinite exterior boundaries. It is observed that the above expression of Green's function is fundamentally different from the "modified Green's function" considered by Mazilu (1972) and Kröner (1990) in which the prescribed displacements or Green's function values on the (finite or infinite) exterior boundaries are homogeneous (zero).

In Eq. (2), $\mathbf{x}'$ defines the ellipsoidal inclusion domain centered at $\mathbf{x}^{(1)}$ as follows:

$$\frac{(x_1' - x_1^{(1)})^2}{a_1^2} + \frac{(x_2' - x_2^{(1)})^2}{a_2^2} + \frac{(x_3' - x_3^{(1)})^2}{a_3^2} \leqslant 1 \tag{4}$$

in which a_i $(i = 1, 2, 3)$ is one of the three semi-axes of the ellipsoid and the center is $\mathbf{x}^{(1)} = (x_1^{(1)}, x_2^{(1)}, x_3^{(1)})$ (Fig. 1(b)).

Following Mura (1987), we can construct a new *imaginary* ellipsoid in terms of Eq. (4) for any point $\mathbf{x}$ within the matrix phase. That is, we have (Fig. 3)

$$\frac{(x_1 - x_1^{(1)})^2}{a_1^2 + \lambda} + \frac{(x_2 - x_2^{(1)})^2}{a_2^2 + \lambda} + \frac{(x_3 - x_3^{(1)})^2}{a_3^2 + \lambda} = 1, \tag{5}$$

where λ is taken as positive ($\lambda > 0$) and can be solved from Eq. (5). Consequently, λ is only a function of $\mathbf{x}$ (in the matrix) and $\mathbf{x}^{(1)}$ (in the real inclusion domain). Moreover, Ju and Sun (1999) introduced the outward unit normal vector $\hat{\mathbf{n}}$ at any matrix point $\mathbf{x}$ on the new imaginary ellipsoid, which can be expressed as (cf. Fig. 3)

$$\hat{n}_i = \frac{x_i - x_i^{(1)}}{(a_I^2 + \lambda)\sqrt{\Theta(\lambda)}} \tag{6}$$

in which

$$\Theta(\lambda) = \Theta_i(\lambda)\Theta_i(\lambda), \tag{7}$$

$$\Theta_i(\lambda) = \frac{x_i - x_i^{(1)}}{a_I^2 + \lambda}. \tag{8}$$

In addition, we follow Mura's (1987) tensorial indicial notation, i.e., repeated lower-case indices are summed up from 1 to 3, whereas upper-case indices take on the same numbers as the corresponding lower-case ones but are not summed up.

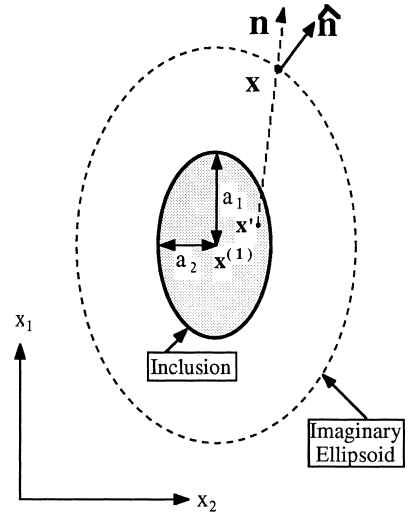

Fig. 3. Schematic representation of the imaginary ellipsoid and its outward unit normal vector $\hat{\mathbf{n}}$.

With the help of the above definitions and after lengthy derivations, the exterior-point Eshelby's tensor $\bar{\mathbf{G}}$ in Eq. (2) can be explicitly expressed in terms of the outward unit normal vector $\hat{\mathbf{n}}$ and the second-rank identity tensor $\mathbf{1}$ (the Kronecker delta tensor) as (cf. Ju and Sun, 1999)

$$\bar{G}_{ijkl}(\mathbf{x}-\mathbf{x}^{(1)}) = \frac{1}{4(1-\nu_0)}\Big[S^{(1)}_{IK}(\lambda)\delta_{ij}\delta_{kl} + S^{(2)}_{IJ}(\lambda)(\delta_{ik}\delta_{jl}+\delta_{il}\delta_{jk}) + S^{(3)}_{I}(\lambda)\delta_{ij}\hat{n}_k\hat{n}_l + S^{(4)}_{K}(\lambda)\delta_{kl}\hat{n}_i\hat{n}_j + S^{(5)}_{I}(\lambda)(\delta_{ik}\hat{n}_j\hat{n}_l+\delta_{il}\hat{n}_j\hat{n}_k) + S^{(6)}_{J}(\lambda)(\delta_{jk}\hat{n}_i\hat{n}_l+\delta_{jl}\hat{n}_i\hat{n}_k) + S^{(7)}_{IJKL}(\lambda)\hat{n}_i\hat{n}_j\hat{n}_k\hat{n}_l\Big], \tag{9}$$

where all the components are given by

$$S^{(1)}_{IK}(\lambda) = -2\nu_0 J_I(\lambda) + \frac{a_I^2}{a_I^2-a_K^2}J_I(\lambda) + \frac{a_K^2}{a_K^2-a_I^2}J_K(\lambda), \tag{10}$$

$$S^{(2)}_{IJ}(\lambda) = -(1-\nu_0)[J_I(\lambda)+J_J(\lambda)] + \frac{a_I^2}{a_I^2-a_J^2}J_I(\lambda) + \frac{a_J^2}{a_J^2-a_I^2}J_J(\lambda), \tag{11}$$

$$S^{(3)}_{I}(\lambda) = 2\rho^3(\lambda)[1-\rho_I^2(\lambda)], \tag{12}$$

$$S^{(4)}_{K}(\lambda) = 2\rho^3(\lambda)[1-2\nu_0-\rho_K^2(\lambda)], \tag{13}$$

$$S^{(5)}_{I}(\lambda) = 2\rho^3(\lambda)[\nu_0-\rho_I^2(\lambda)], \tag{14}$$

$$S^{(6)}_{J}(\lambda) = 2\rho^3(\lambda)[\nu_0-\rho_J^2(\lambda)], \tag{15}$$

$$S^{(7)}_{IJKL}(\lambda) = 2\rho^3(\lambda)\left[2[\rho_I^2(\lambda)+\rho_J^2(\lambda)+\rho_K^2(\lambda)+\rho_L^2(\lambda)] + \rho_m(\lambda)\rho_m(\lambda) - \frac{4\rho_M^2(\lambda)\Theta_m(\lambda)\Theta_m(\lambda)}{\Theta(\lambda)} - 5\right]. \tag{16}$$

Here, $\rho_I(\lambda)$, $\rho(\lambda)$, and $J_I(\lambda)$ are defined as

$$\rho_I(\lambda) = \frac{a_I}{\sqrt{a_I^2+\lambda}}, \tag{17}$$

$$\rho(\lambda) = [\rho_1(\lambda)\rho_2(\lambda)\rho_3(\lambda)]^{1/3}, \tag{18}$$

$$J_I(\lambda) = \int \frac{\rho^3(\lambda)}{a_I^2+\lambda}\mathrm{d}\lambda. \tag{19}$$

It is noticed that the integral $J_I(\lambda)$ can be expressed by the standard elliptic integrals. Further, if the inclusion shape is *spheroidal* ($a_2 = a_3 = a \neq a_1$), then we can integrate the $J_I(\lambda)$ explicitly and therefore obtain the components of the exterior-point Eshelby's tensor. See Appendix A for details. It is noted that Eq. (9) is equivalent to Eq. (11.41) of Mura (1987). However, our treatment is geometrically meaningful (in terms of the new $\hat{\mathbf{n}}$) and features a common indicial structure. Furthermore, our treatment is finished, explicit, compact, systematic, and easy to use in comparison with that of Mura (1987).

In addition, the eigenstrain $\boldsymbol{\epsilon}^{*0}$ in Eq. (1) is given by (cf. Ju and Chen, 1994a)

$$\boldsymbol{\epsilon}^{*0} = -(\mathbf{A}+\mathbf{S})^{-1} : \boldsymbol{\epsilon}^0, \tag{20}$$

where the fourth-rank elastic "phase-mismatch" tensor $\mathbf{A}$ is defined as

$$\mathbf{A} = [\mathbf{C}_1 - \mathbf{C}_0]^{-1} \cdot \mathbf{C}_0 \tag{21}$$

in which $\mathbf{C}_1$ is the linear elasticity tensor of the particle phase. Further, $\mathbf{S}$ is the (interior point) Eshelby's tensor for an ellipsoidal inclusion, which is defined as (Eshelby, 1957):

$$\mathbf{S}(\mathbf{x}-\mathbf{x}^{(1)}) = \int_{\Omega_1(\mathbf{x}^{(1)})} \mathbf{G}(\mathbf{x}-\mathbf{x}')\,\mathrm{d}\mathbf{x}' \tag{22}$$

for $\mathbf{x} \in \Omega_1(\mathbf{x}^{(1)})$.

By comparing Eq. (22) with Eq. (2), we realize that the only difference between the exterior-point Eshelby's tensor $\bar{\mathbf{G}}(\mathbf{x}-\mathbf{x}^{(1)})$ and the (interior point) Eshelby's tensor $\mathbf{S}(\mathbf{x}-\mathbf{x}^{(1)})$ is that the material point $\mathbf{x}$ is inside the *matrix* domain for $\bar{\mathbf{G}}$, whereas $\mathbf{x}$ is in the *inclusion* domain for $\mathbf{S}$. The exterior-point Eshelby's tensor $\bar{\mathbf{G}}$ will not recover the (interior point) Eshelby's tensor $\mathbf{S}$ even as the point $\mathbf{x}$ in the matrix moves to the boundary (interface) between the matrix and the inclusion. The detailed discussions are given in Ju and Sun (1999).

Eshelby (1957) proved that the (interior point) Eshelby's tensor $\mathbf{S}$ does not depend on the location of the point $\mathbf{x}$ in an inclusion. Therefore, $\mathbf{S}$ is a constant tensor. Explicitly, the (interior point) Eshelby's tensor $\mathbf{S}$ for an ellipsoidal inclusion takes the form:

$$S_{ijkl} = \frac{1}{4(1-\nu_0)}[S^{(1)}_{IK}(0)\delta_{ij}\delta_{kl} + S^{(2)}_{IJ}(0)(\delta_{ik}\delta_{jl}+\delta_{il}\delta_{jk})], \tag{23}$$

where $S^{(1)}_{IK}(0)$ and $S^{(2)}_{IJ}(0)$ are special cases of $S^{(1)}_{IK}(\lambda)$ and $S^{(2)}_{IJ}(\lambda)$ in Eqs. (10) and (11) by setting $\lambda = 0$. Moreover, it is clear that the (interior point) Eshelby's tensor depends only on Poisson's ratio of the *matrix* and the three semi-axes of an ellipsoidal inclusion.

Finally, we refer to Appendix A for the explicit expression of the (interior point) Eshelby's tensor corresponding to a spheroidal inclusion. Therefore, upon any external loading, the stress pertubation due to one inhomogeneity can be derived by substituting Eqs. (9) and (20) into Eq. (1).

3. Ensemble-average procedure for PRMMCs

To obtain "effective" constitutive relations of randomly distributed particle-reinforced composites, one typically performs the ensemble-volume averaging procedure (homogenization) within a mesoscopic RVE. Let us consider a two-phase composite containing randomly located yet aligned elastic spheroids embedded in an elastoplastic matrix material. The entire assembly is subjected to specified far-field loadings. Further, all particles are assumed to be non-intersecting (impenetrable) and small deformation is assumed. Hence, the microstructure is assumed to be statistically homogeneous and isotropic with a virtually constant particle volume fraction during the deformation process. For simplicity, the commonly used von Mises J_2-yield criterion with an isotropic hardening law is assumed for the matrix material as an illustration. Extension of the present framework to more general yield criterion and general hardening law can be derived with additional effort.

Accordingly, at any matrix material point $\mathbf{x}$, the stress $\boldsymbol{\sigma}(\mathbf{x})$ must satisfy the following yield function:

$$F(\boldsymbol{\sigma}, \bar{\mathrm{e}}^{\mathrm{p}}_m) = \sqrt{\boldsymbol{\sigma} : \mathbf{I}_{\mathrm{d}} : \boldsymbol{\sigma}} - K(\bar{\mathrm{e}}^{\mathrm{p}}_m) \leqslant 0 \tag{24}$$

in which $\bar{\mathrm{e}}^{\mathrm{p}}_m$ and $K(\bar{\mathrm{e}}^{\mathrm{p}}_m)$, respectively, are the equivalent plastic strain and the isotropic hardening function of the matrix-only material. Extension can be made to accommodate the kinematic hardening law. Moreover, $\mathbf{I}_{\mathrm{d}}$ denotes the deviatoric part of the fourth-rank identity tensor $\mathbf{I}$, i.e.,

$$\mathbf{I}_{\mathrm{d}} = \mathbf{I} - \tfrac{1}{3}\mathbf{1}\otimes\mathbf{1}. \tag{25}$$

Following Ju and Chen (1994c) and Ju and Tseng (1996), we denote by $H(\mathbf{x}|\mathscr{G})$ the square of the "current stress norm" at a local point $\mathbf{x}$, which contributes to the plastic yielding criterion of PRMMCs for a given particle configuration (assembly) $\mathscr{G}$. As there is no plastic deformation in the elastic particles, $H(\mathbf{x}|\mathscr{G})$ can be written as

$$H(\mathbf{x}|\mathscr{G}) = \begin{cases} \boldsymbol{\sigma}(\mathbf{x}|\mathscr{G}) : \mathbf{I}_{\mathrm{d}} : \boldsymbol{\sigma}(\mathbf{x}|\mathscr{G}) & \text{if } \mathbf{x} \text{ in the matrix,} \\ 0 & \text{otherwise.} \end{cases} \tag{26}$$

We now define $\langle H \rangle_m(\mathbf{x})$ as the ensemble average of $H(\mathbf{x}|\mathscr{G})$ over all possible realizations for a matrix point $\mathbf{x}$. Further, we define $P(\mathscr{G})$ as the probability density function for finding a particle configuration $\mathscr{G}$ in the composite. Accordingly, $\langle H \rangle_m(\mathbf{x})$ can be expressed as

$$\langle H \rangle_m(\mathbf{x}) = H^0 + \int_{\mathscr{G}} \left\{ H(\mathbf{x}|\mathscr{G}) - H^0 \right\} \mathrm{P}(\mathscr{G})\, \mathrm{d}\mathscr{G}, \tag{27}$$

where H^0 is the square of the far-field stress norm in the matrix,

$$H^0 = \boldsymbol{\sigma}^0 : \mathbf{I}_{\mathrm{d}} : \boldsymbol{\sigma}^0. \tag{28}$$

The expression for $\langle H \rangle_m(\mathbf{x})$ can be approximately obtained by neglecting the interaction among neighboring particles. This process is illustrated in Fig. 4. That is, a matrix point $\mathbf{x}$ simply collects the perturbation from all randomly located, non-interacting particles

$$\langle H \rangle_m(\mathbf{x}) \cong H^0 + \int_{\mathbf{x}^{(1)} \notin \Xi(\mathbf{x})} \left\{ H(\mathbf{x}|\mathbf{x}^{(1)}) - H^0 \right\} \mathrm{P}(\mathbf{x}^{(1)})\, \mathrm{d}\mathbf{x}^{(1)} + \cdots +, \tag{29}$$

where $\Xi(\mathbf{x})$ is the "exclusion zone" of $\mathbf{x}$ for the center location $\mathbf{x}^{(1)}$ of a particle in the *probability* space, which is identical to the shape and size of a spheroidal particle. The probabilistic exclusion zone states that $\mathbf{x}^{(1)}$ cannot be located within the $\Xi(\mathbf{x})$ domain because $\mathbf{x}$ must be located within the matrix phase. In addition, $\mathrm{P}(\mathbf{x}^{(1)})$ denotes the probability density function for finding a particle centered at $\mathbf{x}^{(1)}$. Here, $\mathrm{P}(\mathbf{x}^{(1)})$ is assumed to be statistically homogeneous, isotropic and uniform. Therefore, we write $\mathrm{P}(\mathbf{x}^{(1)}) = N/V$ where N is the total number of particles dispersed in an RVE V. As the exclusion zone is very small (one particle domain) compared with the infinitely large probability space, it is reasonable to approximate the tiny spheroidal exclusion zone by an equal-volume spherical exclusion zone. Namely, we define an equal-

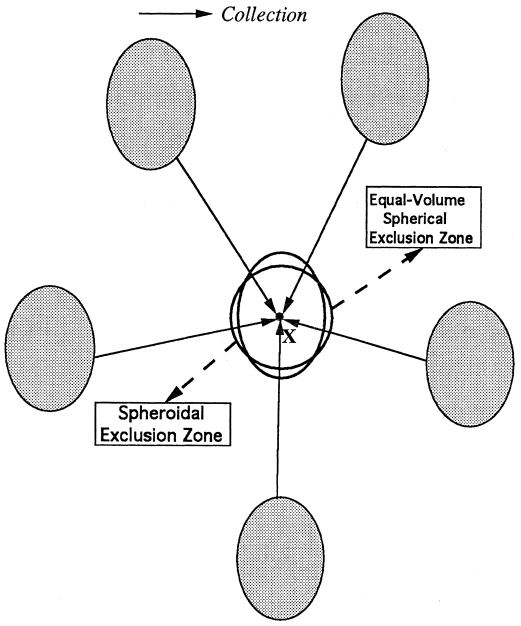

Fig. 4. A local matrix point $\mathbf{x}$ collecting perturbations from the surrounding particles, with a tiny probabilistic exclusion zone.

volume spherical probabilistic exclusion zone with the radius $a^* = (a_1 a_2^2)^{1/3} = a_1/\alpha^{2/3}$, where $\alpha = a_1/a_2$ is the aspect ratio of a spheroid. Accordingly, Eq. (29) can be recast into an approximate form

$$\langle H \rangle_m \cong H^0 + \frac{N}{V} \int_{a^*}^{\infty} \mathrm{d}r \int_{A(r)} \left\{ H(r) - H^0 \right\} \mathrm{d}A + \cdots +, \tag{30}$$

where $A(r)$ is a surface of radius $r = \|\mathbf{x} - \mathbf{x}^{(1)}\|$ in the probability space. Despite the approximation involving a^*, the integrand $H(r)$ preserves the *spheroidal* $\hat{\mathbf{n}}$ and $\mathbf{S}$, which are functions of the aspect ratio α.

Upon integrating the above surface integral, we discover the following two identities involving spheroidal $\hat{\mathbf{n}}$:

$$\int_{A(r)} \hat{n}_i \hat{n}_j \, \mathrm{d}A = \frac{4\pi r^2}{3} \Delta_I \delta_{ij}, \tag{31}$$

$$\int_{A(r)} \hat{n}_i \hat{n}_j \hat{n}_k \hat{n}_l \, \mathrm{d}A = \frac{4\pi r^2}{15} \left[\Delta_{IK} \delta_{ij} \delta_{kl} + \Delta_{IJ} (\delta_{ik} \delta_{jl} + \delta_{il} \delta_{jk}) \right], \tag{32}$$

where the components of Δ_I and Δ_{IJ} read

$$\Delta_1 = \frac{3[1 - \alpha^4 f(\alpha^2)]}{1 - \alpha^4}, \tag{33}$$

$$\Delta_2 = \Delta_3 = \tfrac{1}{2}(3 - \Delta_1), \tag{34}$$

$$[\Delta_{IJ}] = \begin{bmatrix} b & c & c \\ c & d & d \\ c & d & d \end{bmatrix} \tag{35}$$

with

$$f(\alpha) = \begin{cases} \frac{\cos^{-1}\alpha}{\alpha\sqrt{1-\alpha^2}}, & \alpha < 1, \\ \frac{\cosh^{-1}\alpha}{\alpha\sqrt{\alpha^2-1}}, & \alpha > 1, \end{cases} \tag{36}$$

$$b = \frac{5}{2(1 - \alpha^4)^2} [2 + \alpha^4 - 3\alpha^4 f(\alpha^2)], \tag{37}$$

$$c = \frac{15\alpha^4}{4(1 - \alpha^4)^2} [-3 + (1 + 2\alpha^4) f(\alpha^2)], \tag{38}$$

$$d = \tfrac{1}{8}(15 - 3b - 4c). \tag{39}$$

In addition, Sun (1998) derived an explicit novel inverse formula for the fourth-rank "generalized isotropic" tensor, which is given in Appendix B.

With the help of the above tools and by dropping some higher-order terms, we can evaluate the ensemble-averaged square of the current stress norm at any matrix point as

$$\langle H \rangle_m \cong \boldsymbol{\sigma}^0 : \mathbf{T} : \boldsymbol{\sigma}^0, \tag{40}$$

where the components of the fourth-rank tensor $\mathbf{T}$ take the form:

$$T_{ijkl} = T_{IK}^{(1)} \delta_{ij} \delta_{kl} + T_{IJ}^{(2)} (\delta_{ik} \delta_{jl} + \delta_{il} \delta_{jk}) \tag{41}$$

with

$$T_{IK}^{(1)} = -\frac{1}{3} + \frac{2\phi}{4725(1-v_0)^2 B_{II} B_{KK}} \Big[1575(1-2v_0)^2 \Gamma_{II}\Gamma_{KK} + 21(25v_0-23)(1-2v_0) \times(\Gamma_{II}\Delta_K + \Gamma_{KK}\Delta_I) + 21(25v_0-2)(1-2v_0)(\Gamma_{II}+\Gamma_{KK}) + 3(35v_0^2-70v_0+36)\Delta_{IK} + 7(50v_0^2-59v_0+8)(\Delta_I+\Delta_K) - 2(175v_0^2-343v_0+103)\Big], \tag{42}$$

$$T_{IJ}^{(2)} = \frac{1}{2} + \frac{\phi}{1575(1-v_0)^2 B_{IJ} B_{IJ}} \Big[(72-140v_0+70v_0^2)\Delta_{IJ} - (75-266v_0+175v_0^2)\frac{\Delta_I+\Delta_J}{2} + 164-476v_0+350v_0^2\Big]. \tag{43}$$

Here, ϕ is the volume fraction of particles, which is defined as $\phi = (4\pi a_1^3/3\alpha^2)(N/V)$. Further, we have

$$B_{IJ} = 2[Z_2 + S_{IJ}^{(2)}(0)], \tag{44}$$

$$\Gamma_{I1} = \frac{[2Z_1 + 2S_{22}^{(1)}(0) + B_{22}][Z_1 + S_{I1}^{(1)}(0)] - 2[Z_1 + S_{21}^{(1)}(0)][Z_1 + S_{I2}^{(1)}(0)]}{[2Z_1 + 2S_{22}^{(1)}(0) + B_{22}][Z_1 + S_{11}^{(1)}(0) + B_{11}] - 2[Z_1 + S_{12}^{(1)}(0)][Z_1 + S_{21}^{(1)}(0)]}, \tag{45}$$

$$\Gamma_{I2} = \Gamma_{I3} = \frac{[Z_1 + S_{11}^{(1)}(0) + B_{11}][Z_1 + S_{I2}^{(1)}(0)] - [Z_1 + S_{12}^{(1)}(0)][Z_1 + S_{I1}^{(1)}(0)]}{[2Z_1 + 2S_{22}^{(1)}(0) + B_{22}][Z_1 + S_{11}^{(1)}(0) + B_{11}] - 2[Z_1 + S_{12}^{(1)}(0)][Z_1 + S_{21}^{(1)}(0)]}, \tag{46}$$

where

$$Z_1 = \frac{\lambda_0\mu_1 - \lambda_1\mu_0}{(\mu_1-\mu_0)[2(\mu_1-\mu_0) + 3(\lambda_1-\lambda_0)]}, \tag{47}$$

$$Z_2 = \frac{\mu_0}{2(\mu_1-\mu_0)} \tag{48}$$

and λ_β and μ_β are the Lame constants of the β-phase ($\beta = 0, 1$).

It is interesting to observe that if one allows the particle volume fraction ϕ to go to zero in Eqs. (42) and (43), the tensor $\mathbf{T}$ then reduces to the fourth-rank deviatoric identity tensor $\mathbf{I}_d$. Consequently, the ensemble-averaged square of the stress norm defined in Eq. (40) reduces to the second deviatoric stress invariant J_2, which is employed to define the classical von Mises yield criterion. Within the present formulation, the effect of the spheroidal aspect ratio α upon the ensemble-averaged square of the current stress norm $\langle H\rangle_m$ is preserved through the effective radius a^*, the outer normal $\hat{\mathbf{n}}$, and the spheroidal (interior point) Eshelby's tensor $\mathbf{S}$.

In Eq. (40), $\langle H\rangle_m$ is described in terms of the far-field stress $\boldsymbol{\sigma}^0$. Alternatively, the ensemble-averaged square of the current stress norm can be expressed in terms of the macroscopic (ensemble-volume averaged) stress $\bar{\boldsymbol{\sigma}}$. The relationship between the far-field stress $\boldsymbol{\sigma}^0$ and the macroscopic stress $\bar{\boldsymbol{\sigma}}$ is given by (cf. Ju and Chen, 1994a,c)

$$\boldsymbol{\sigma}^0 = \mathbf{P} : \bar{\boldsymbol{\sigma}}, \tag{49}$$

where the fourth-rank tensor $\mathbf{P}$ reads

$$\mathbf{P} = \{\mathbf{C}_0 \cdot [\mathbf{I} + \phi(\mathbf{I}-\mathbf{S}) \cdot (\mathbf{A}+\mathbf{S})^{-1}] \cdot \mathbf{C}_0^{-1}\}^{-1}. \tag{50}$$

With the help of the inverse formula for the "generalized isotropic" fourth-rank tensor provided in Appendix B, $\mathbf{P}$ can be expressed as

$$P_{ijkl} = P_{IK}^{(1)}\delta_{ij}\delta_{kl} + P_{IJ}^{(2)}(\delta_{ik}\delta_{jl} + \delta_{il}\delta_{jk}) \tag{51}$$

with

$$P_{IK}^{(1)} = -\frac{\Gamma_{IK}^{(3)}}{2\Gamma_{II}^{(2)}}, \tag{52}$$

$$P_{IJ}^{(2)} = \frac{1}{4\Gamma_{IJ}^{(2)}}, \tag{53}$$

where

$$\Gamma_{I1}^{(3)} = \frac{(\Gamma_{22}^{(1)} + \Gamma_{22}^{(2)})\Gamma_{I1}^{(1)} - \Gamma_{21}^{(1)}\Gamma_{I2}^{(1)}}{(\Gamma_{11}^{(1)} + 2\Gamma_{11}^{(2)})(\Gamma_{22}^{(1)} + \Gamma_{22}^{(2)}) - \Gamma_{12}^{(1)}\Gamma_{21}^{(1)}}, \tag{54}$$

$$\Gamma_{I2}^{(3)} = \Gamma_{I3}^{(3)} = \frac{(\Gamma_{11}^{(1)} + 2\Gamma_{11}^{(2)})\Gamma_{I2}^{(1)} - \Gamma_{12}^{(1)}\Gamma_{I1}^{(1)}}{2(\Gamma_{11}^{(1)} + 2\Gamma_{11}^{(2)})(\Gamma_{22}^{(1)} + \Gamma_{22}^{(2)}) - 2\Gamma_{12}^{(1)}\Gamma_{21}^{(1)}}, \tag{55}$$

$$\Gamma_{IJ}^{(2)} = \frac{1}{2} + \frac{(1 - 2S_{IJ}^{(2)})\phi}{2B_{IJ}}, \tag{56}$$

$$\Gamma_{IK}^{(1)} = \phi\left[\frac{\Gamma_{mK}S_{Im}^{(1)}}{B_{MM}} - \frac{S_{IK}^{(1)}}{B_{KK}} - \frac{\Gamma_{IK}(1 - 2S_{II}^{(2)})}{B_{II}}\right]. \tag{57}$$

Combination of Eqs. (49) and (40) then leads to the alternative expression for the ensemble-averaged square of the current stress norm as

$$\langle H\rangle_m = \bar{\boldsymbol{\sigma}} : \bar{\mathbf{T}} : \bar{\boldsymbol{\sigma}}, \tag{58}$$

where the fourth-rank tensor $\bar{\mathbf{T}}$ is defined as

$$\bar{\mathbf{T}} = \mathbf{P}^{\mathrm{T}} \cdot \mathbf{T} \cdot \mathbf{P}. \tag{59}$$

After carrying out the lengthy algebra, the components of $\bar{\mathbf{T}}$ are explicitly given by

$$\bar{T}_{ijkl} = \bar{T}_{IK}^{(1)}\delta_{ij}\delta_{kl} + \bar{T}_{IJ}^{(2)}(\delta_{ik}\delta_{jl} + \delta_{il}\delta_{jk}), \tag{60}$$

where

$$\begin{aligned}\bar{T}_{IK}^{(1)} = {} & 4P_{II}^{(2)}T_{II}^{(2)}P_{IK}^{(1)} + 4P_{KK}^{(2)}T_{KK}^{(2)}P_{KI}^{(1)} + 4P_{II}^{(2)}T_{IK}^{(1)}P_{KK}^{(2)} + 2P_{II}^{(2)}T_{Im}^{(1)}P_{mK}^{(1)} + 2P_{KK}^{(2)}T_{mK}^{(1)}P_{mI}^{(1)} + 2P_{mK}^{(1)}T_{MM}^{(2)}P_{mI}^{(1)} \\ & + P_{mK}^{(1)}T_{nm}^{(1)}P_{nI}^{(1)},\end{aligned} \tag{61}$$

$$\bar{T}_{IJ}^{(2)} = 4P_{IJ}^{(2)}T_{IJ}^{(2)}P_{IJ}^{(2)}. \tag{62}$$

It is observed again that the ensemble-averaged square of the current stress norm given in Eq. (58) reduces to the classical J_2-invariant upon substituting $\phi = 0$ into Eqs. (61) and (62). Therefore, the tensor $\bar{\mathbf{T}}$ reduces to the fourth-rank deviatoric identity tensor $\mathbf{I}_{\mathrm{d}}$ for $\phi = 0$.

As shown by Ju and Chen (1994a,c), the tensor $\mathbf{P}$ in Eq. (50) accounts for the far-field interaction effect of particles. That is, although the near-field direct particle interactions are not considered, the interactions between particles and the far-field boundary are included in the tensor $\mathbf{P}$. In fact, Ju and Chen (1994a) showed that the elastic far-field interaction formulation (the so-called *non-interacting* formulation therein) renders identical elastic moduli to those obtained by the variational bounds of Willis (1977) and the

Mori-Tanaka formulation of Weng (1990) for elastic composites with aligned ellipsoidal inclusions. Therefore, $\langle H\rangle_m$ in Eq. (58) contains the far-field interaction effect.

In Section 4, we will propose the effective yield function and derive the overall elastoplastic constitutive behavior of aligned spheroid-reinforced MMCs in accordance with the formulas derived in this section.

4. The effective elastoplastic constitutive behavior of PRMMCs

According to the continuum plasticity, the total macroscopic strain $\bar{\boldsymbol{\epsilon}}$ is assumed to consist of two parts:

$$\bar{\boldsymbol{\epsilon}} = \bar{\boldsymbol{\epsilon}}^{\mathrm{e}} + \bar{\boldsymbol{\epsilon}}^{\mathrm{p}}, \tag{63}$$

where $\bar{\boldsymbol{\epsilon}}^{\mathrm{e}}$ denotes the macroscopic elastic strain and $\bar{\boldsymbol{\epsilon}}^{\mathrm{p}}$ represents the macroscopic plastic strain of PRMMCs. The relationship between the macroscopic stress $\bar{\boldsymbol{\sigma}}$ and the macroscopic elastic strain reads

$$\bar{\boldsymbol{\sigma}} = \mathbf{C}^* : \bar{\boldsymbol{\epsilon}}^{\mathrm{e}}, \tag{64}$$

where the effective elastic stiffness tensor $\mathbf{C}^*$ (with the far-field interaction effect) of the aligned ellipsoid-reinforced two-phase MMCs takes the form (cf. Ju and Chen, 1994a):

$$\mathbf{C}^* = \mathbf{C}_0 + \phi\mathbf{C}_0 \cdot [\mathbf{A} + (1-\phi)\mathbf{S}]^{-1}. \tag{65}$$

In the case of aligned (in the x_1-direction) spheroid-reinforced MMCs, by using the inversion formula in Appendix B, $\mathbf{C}^*$ can be explicitly expressed as

$$C^*_{ijkl} = C^{(1)}_{IK}\delta_{ij}\delta_{kl} + C^{(2)}_{IJ}(\delta_{ik}\delta_{jl} + \delta_{il}\delta_{jk}), \tag{66}$$

where

$$C^{(1)}_{IK} = \lambda_0 - 2\mu_0\phi\frac{\Psi_{IK}}{\psi_{II}} + \frac{\lambda_0\phi}{\psi_{KK}} - \lambda_0\phi\sum_{m=1}^{3}\frac{\Psi_{mK}}{\psi_{mm}}, \tag{67}$$

$$C^{(2)}_{IJ} = \mu_0\left(1 + \frac{\phi}{\psi_{IJ}}\right) \tag{68}$$

with

$$\psi_{IJ} = 2[Z_2 + (1-\phi)S^{(2)}_{IJ}], \tag{69}$$

$$\Psi_{I1} = \frac{\xi_2[Z_1 + (1-\phi)S^{(1)}_{I1}(0)] - 2\xi_4[Z_1 + (1-\phi)S^{(1)}_{I2}(0)]}{\xi_1\xi_2 - 2\xi_3\xi_4}, \tag{70}$$

$$\Psi_{I2} = \Psi_{I3} = \frac{\xi_1[Z_1 + (1-\phi)S^{(1)}_{I2}(0)] - \xi_3[Z_1 + (1-\phi)S^{(1)}_{I1}(0)]}{\xi_1\xi_2 - 2\xi_3\xi_4}, \tag{71}$$

$$\xi_1 = Z_1 + (1-\phi)S^{(1)}_{11}(0) + \psi_{11}, \tag{72}$$

$$\xi_2 = 2Z_1 + 2(1-\phi)S^{(1)}_{22}(0) + \psi_{22}, \tag{73}$$

$$\xi_3 = Z_1 + (1-\phi)S^{(1)}_{12}(0), \tag{74}$$

$$\xi_4 = Z_1 + (1-\phi)S^{(1)}_{21}(0). \tag{75}$$

It is easy to show that $C^{(1)}_{12} = C^{(1)}_{13}, C^{(1)}_{21} = C^{(1)}_{31}, C^{(1)}_{22} = C^{(1)}_{23} = C^{(1)}_{32} = C^{(1)}_{33}, C^{(2)}_{12} = C^{(2)}_{21} = C^{(2)}_{13} = C^{(2)}_{31}$, $C^{(2)}_{22} = C^{(2)}_{33} = C^{(2)}_{23} = C^{(2)}_{32}$. In addition, in spite of the lack of major symmetry for the (interior point) Eshelby's tensor of spheroidal inclusion, it can be proved that $C^{(1)}_{12} = C^{(1)}_{21}$.

Therefore, as expected, the overall elasticity tensor $\mathbf{C}^*$ in Eq. (66) for an aligned spheroid-reinforced composite exhibits transverse isotropy. Alternatively, by means of the engineering matrix form, the effective elastic constitutive relation can be rephrased as

$$\{\bar{\sigma}_i\} = [C^*_{ij}]\{\bar{\epsilon}^{\mathrm{e}}_j\}, \tag{76}$$

where

$$\{\bar{\sigma}_i\} = \{\bar{\sigma}_{11}, \bar{\sigma}_{22}, \bar{\sigma}_{33}, \bar{\sigma}_{23}, \bar{\sigma}_{31}, \bar{\sigma}_{12}\}^{\mathrm{T}}, \tag{77}$$

$$\{\bar{\epsilon}^{\mathrm{e}}_j\} = \{\bar{\epsilon}^{\mathrm{e}}_{11}, \bar{\epsilon}^{\mathrm{e}}_{22}, \bar{\epsilon}^{\mathrm{e}}_{33}, 2\bar{\epsilon}^{\mathrm{e}}_{23}, 2\bar{\epsilon}^{\mathrm{e}}_{31}, 2\bar{\epsilon}^{\mathrm{e}}_{12}\}^{\mathrm{T}}, \tag{78}$$

and the transversely isotropic stiffness matrix $[C^*_{ij}]$ becomes

$$[C^*_{ij}] = \begin{bmatrix} C^{(1)}_{11} + 2C^{(2)}_{11} & C^{(1)}_{12} & C^{(1)}_{12} & 0 & 0 & 0 \\ C^{(1)}_{12} & C^{(1)}_{22} + 2C^{(2)}_{22} & C^{(1)}_{22} & 0 & 0 & 0 \\ C^{(1)}_{12} & C^{(1)}_{22} & C^{(1)}_{22} + 2C^{(2)}_{22} & 0 & 0 & 0 \\ 0 & 0 & 0 & C^{(2)}_{22} & 0 & 0 \\ 0 & 0 & 0 & 0 & C^{(2)}_{12} & 0 \\ 0 & 0 & 0 & 0 & 0 & C^{(2)}_{12} \end{bmatrix}. \tag{79}$$

Here, the axis of axisymmetry is parallel to the x_1-axis. Apparently, the overall elastic response can be described by the five elastic constants: $[C^{(1)}_{11} + 2C^{(2)}_{11}], C^{(1)}_{12}, C^{(1)}_{22}, C^{(2)}_{22}$, and $C^{(2)}_{12}$. The requirement $C^*_{44} = (C^*_{22} - C^*_{23})/2$ can be easily verified for the present problem.

Upon loading, the two-phase PRMMCs may yield and become plastic. The ensemble- and volume-averaged "current stress norm" for a particulate composite can be micromechanically derived as

$$\sqrt{\langle H \rangle} = (1-\phi)\sqrt{\bar{\boldsymbol{\sigma}} : \bar{\mathbf{T}} : \bar{\boldsymbol{\sigma}}}. \tag{80}$$

It is recalled that ϕ denotes the volume fraction of particles. As a result, the macroscopic yield function for an aligned spheroid-reinforced MMC can be characterized by

$$\bar{F} = (1-\phi)\sqrt{\bar{\boldsymbol{\sigma}} : \bar{\mathbf{T}} : \bar{\boldsymbol{\sigma}}} - K(\bar{\mathrm{e}}^{\mathrm{p}}) \leqslant 0 \tag{81}$$

where the simple isotropic hardening function $K(\bar{\mathrm{e}}^{\mathrm{p}})$ is proposed as

$$K(\bar{\mathrm{e}}^{\mathrm{p}}) = \sqrt{\tfrac{2}{3}}\left\{\sigma_{\mathrm{y}} + h(\bar{\mathrm{e}}^{\mathrm{p}})^{\mathrm{q}}\right\}. \tag{82}$$

Here, σ_{y} denotes the initial yield stress, h and q signify the linear and exponential isotropic hardening parameters, respectively, and $\bar{\mathrm{e}}^{\mathrm{p}}$ defines the effective equivalent plastic strain. It is emphasized that the overall yield function is *pressure dependent* and not of the von Mises type any more.

Moreover, for simplicity, the overall ensemble volume averaged flow rule is assumed to be associative. Extension to non-associative flow rule can be constructed in a similar manner. Accordingly, the plastic strain rate for PRMMCs takes the form:

$$\dot{\bar{\boldsymbol{\epsilon}}}^{\mathrm{p}} = \dot{\lambda}\frac{\partial \bar{F}}{\partial \bar{\boldsymbol{\sigma}}} = (1-\phi)\dot{\lambda}\frac{\bar{\mathbf{T}} : \bar{\boldsymbol{\sigma}}}{\sqrt{\bar{\boldsymbol{\sigma}} : \bar{\mathbf{T}} : \bar{\boldsymbol{\sigma}}}}, \tag{83}$$

where $\dot{\lambda}$ is the plastic consistency parameter. Substituting Eq. (60) into the above formula, the overall plastic strain rate can be rephrased as

$$\dot{\bar{\epsilon}}^{\mathrm{p}}_{ij} = (1-\phi)\dot{\lambda}\frac{[\bar{T}^{(1)}_{IK}\bar{\sigma}_{kk}]\delta_{ij} + 2\bar{T}^{(2)}_{IJ}\bar{\sigma}_{ij}}{\sqrt{[\bar{T}^{(1)}_{MN}\bar{\sigma}_{mm}\bar{\sigma}_{nn}] + 2\bar{T}^{(2)}_{MN}\bar{\sigma}_{mn}\bar{\sigma}_{mn}}}. \tag{84}$$

Further, the effective equivalent plastic strain rate for PRMMCs is defined as

$$\dot{\bar{\epsilon}}^{\mathrm{p}} = \sqrt{\tfrac{2}{3}\dot{\bar{\epsilon}}^{\mathrm{p}} : \bar{\mathbf{T}}^{-1} : \dot{\bar{\boldsymbol{\epsilon}}}^{\mathrm{p}}} = \sqrt{\tfrac{2}{3}}(1-\phi)\dot{\lambda}, \tag{85}$$

$\dot{\lambda}$ together with the yield function $\bar{F}$ must obey the Kuhn–Tucker loading and unloading conditions. From the plastic consistency condition, $\dot{\lambda}$ can be calculated as

$$\dot{\lambda} = \frac{\frac{\partial \bar{F}}{\partial \bar{\boldsymbol{\sigma}}} : \mathbf{C}^{*} : \dot{\bar{\boldsymbol{\epsilon}}}}{\frac{1-\phi}{\sqrt{\bar{\boldsymbol{\sigma}}:\bar{\mathbf{T}}:\bar{\boldsymbol{\sigma}}}}\left[\frac{\partial \bar{F}}{\partial \bar{\boldsymbol{\sigma}}} : (\mathbf{C}^{*}\cdot\bar{\mathbf{T}}) : \bar{\boldsymbol{\sigma}}\right] - \left[\sqrt{\tfrac{2}{3}}(1-\phi)\frac{\partial \bar{F}}{\partial \bar{\epsilon}^{\mathrm{p}}}\right]}. \tag{86}$$

Accordingly, the relationship between the overall strain rate tensor and the overall stress rate tensor is recast as

$$\dot{\bar{\boldsymbol{\sigma}}} = \mathbf{C}^{*\mathrm{ep}} : \dot{\bar{\boldsymbol{\epsilon}}}, \tag{87}$$

where the elastoplastic continuum tangent stiffness tensor $\mathbf{C}^{*\mathrm{ep}}$ takes the form

$$\mathbf{C}^{*\mathrm{ep}} = \begin{cases} \mathbf{C}^{*} & \text{if } \dot{\lambda} = 0 \text{ (elastic)}, \\ \mathbf{C}^{*}\cdot(\mathbf{I}-\mathbf{U}) & \text{if } \dot{\lambda} > 0 \text{ (plastic)}. \end{cases} \tag{88}$$

Here, the fourth-rank tensor $\mathbf{U}$ satisfies $\dot{\bar{\epsilon}}^{\mathrm{p}} = \mathbf{U} : \dot{\bar{\boldsymbol{\epsilon}}}$ and reads

$$\mathbf{U} = \frac{(\bar{\mathbf{T}} : \bar{\boldsymbol{\sigma}}) \otimes (\mathbf{C}^{*}\cdot\bar{\mathbf{T}} : \bar{\boldsymbol{\sigma}})}{\bar{\boldsymbol{\sigma}} : \left[\bar{\mathbf{T}}\cdot\mathbf{C}^{*}\cdot\bar{\mathbf{T}} + \frac{2hq(\bar{\epsilon}^{\mathrm{p}})^{q-1}}{3(1-\phi)}\bar{\mathbf{T}}\right] : \bar{\boldsymbol{\sigma}}}. \tag{89}$$

It is noted that $\mathbf{U}$ is non-symmetric but $\mathbf{C}^{*\mathrm{ep}}$ is symmetric.

5. Conclusion

Emanating from the "eigenstrain concept" of *micromechanics* and the macroscopic *homogenization*, the ensemble volume averaged elastoplastic constitutive equations are derived for two-phase metal matrix composites containing randomly dispersed, unidirectionally aligned elastic spheroidal particles. The "far-field interacting" stress perturbation formulation is presented based on the probabilistic spatial distribution, the aspect ratio, and the volume fraction of spheroidal particles, as well as the mechanical properties of constituent phases. The interior-point and exterior-point Eshelby's tensors for spheroidal inclusions are employed to arrive at the proposed derivations. The elastoplastic behavior of PRMMCs is characterized by the *micromechanically* derived effective yield function together with the *illustrative* overall associative plastic flow rule and the isotropic hardening law under three-dimensional loading and unloading histories.

In the present study, we have micromechanically derived the overall yield function, which is quadratic, but not of the von Mises J_2-type any more. However, in general, this form may not be universal for all MMCs. For example, Hashin (1980) and Dvorak et al. (1988), based on phenomenological continuum plasticity, suggested that the overall yield function of anisotropic *fibrous* composites be constructed from piecewise smooth sections and not from a single smooth surface. In addition, in the case of *laminated* composites, deBotton and Ponte Castaneda (1992) derived the functional form of the effective yield function, which is different from that of the constituent phases. We would need to consider tensile particle fracture mode, tensile interfacial particle/matrix debonding mode, compressive particle mode, tensile matrix

failure mode, and compressive matrix failure mode, for example, in order to render a sophisticated multi-surface piecewise smooth damage-plasticity model. Further, more general isotropic/kinematic hardening laws and alternative non-associative flow rule can be considered within the proposed framework based on reliable experimental data and evidence (if available); see, e.g., Dvorak et al. (1988) for kinematic hardening law and non-associative flow rule for fibrous boron-aluminum composite. These issues can be further investigated within the proposed context in the future, but with considerably more effort. It is noted, however, that the present paper does not purport to include all phenomenological continuum plasticity aspects or features. Instead, we apply the micromechanical and ensemble-volume average methodology to the simple J_2-type plastic yield function with the power-law isotropic hardening rule and the associative flow rule as an illustration of the proposed concept and framework. In addition, we have not considered the effect of interfacial particle/matrix debonding upon the overall elastoplastic behavior.

In a related paper (Sun and Ju, 2000), we will present applications of the proposed formulation to uniaxial stress–strain behavior of spheroid-reinforced MMCs, the behavior of PRMMCs under the purely hydrostatic tension, the axisymmetric stress–strain behavior, and the initial yield surfaces for MMCs and porous ductile materials. In addition, the extension to elasto-viscoplastic behavior of PRMMCs will also be addressed in Sun and Ju (2000). Nevertheless, care should be exercised in terms of the range of the aspect ratio α and the particle volume fraction ϕ. We recall that the effect of the aspect ratio of spheroidal particles on the overall elastoplastic behavior is preserved through a^*, $\hat{\mathbf{n}}$ and $\mathbf{S}$. Moreover, the near-field direct particle interactions are not included, although the far-field interactions are accounted for. Therefore, the current model should avoid extreme values for the aspect ratio, and avoid high particle volume fractions.

Acknowledgements

This work was sponsored by the National Science Foundation, Mechanics and Materials Program, under the PYI Grant MSS-9157238. This support is gratefully acknowledged. In addition, the authors are grateful to the very helpful comments provided by two reviewers.

Appendix A. Components of the exterior- and interior-point Eshelby's tensors for a spheroidal inclusion

For a spheroidal inclusion aligned with the x_1-axis, the explicit formulas for the first two components $\mathbf{S}^{(1)}(\lambda)$ and $\mathbf{S}^{(2)}(\lambda)$ of the exterior-point Eshelby's tensor can be expressed as

$$S_{11}^{(1)}(\lambda) = \left[-4v_0 - \frac{2}{\alpha^2-1}\right] g(\lambda) - \frac{2}{3(\alpha^2-1)}\rho_1^3(\lambda) + \left[4v_0 + \frac{2}{\alpha^2-1}\right]\rho_1(\lambda)\rho_2^2(\lambda), \tag{A.1}$$

$$S_{12}^{(1)}(\lambda) = S_{13}^{(1)}(\lambda) = \left[-4v_0 + \frac{2\alpha^2+1}{\alpha^2-1}\right] g(\lambda) + \left[4v_0 - \frac{2\alpha^2}{\alpha^2-1}\right]\rho_1(\lambda)\rho_2^2(\lambda), \tag{A.2}$$

$$S_{21}^{(1)}(\lambda) = S_{31}^{(1)}(\lambda) = \left[-2v_0 - \frac{2\alpha^2+1}{\alpha^2-1}\right] g(\lambda) - \frac{2\alpha^2}{\alpha^2-1}\rho_1(\lambda)\rho_2^2(\lambda), \tag{A.3}$$

$$S_{22}^{(1)}(\lambda) = S_{23}^{(1)}(\lambda) = S_{32}^{(1)}(\lambda) = S_{33}^{(1)}(\lambda) = \left[-2v_0 + \frac{4\alpha^2-1}{4(\alpha^2-1)}\right] g(\lambda) + \frac{\alpha^2}{2(\alpha^2-1)}\frac{\rho_2^4(\lambda)}{\rho_1(\lambda)}, \tag{A.4}$$

$$S_{11}^{(2)}(\lambda) = \left[-4v_0 + \frac{4\alpha^2-2}{\alpha^2-1}\right] g(\lambda) - \frac{2}{3(\alpha^2-1)}\rho_1^3(\lambda) - \left[4v_0 - \frac{4\alpha^2-2}{\alpha^2-1}\right]\rho_1(\lambda)\rho_2^2(\lambda), \tag{A.5}$$

$$S_{12}^{(2)}(\lambda)=S_{13}^{(2)}(\lambda)=S_{21}^{(2)}(\lambda)=S_{31}^{(2)}(\lambda)=\left[-v_0-\frac{\alpha^2+2}{\alpha^2-1}\right]g(\lambda)-\left[2v_0+\frac{2}{\alpha^2-1}\right]\rho_1(\lambda)\rho_2^2(\lambda), \tag{A.6}$$

$$S_{22}^{(2)}(\lambda)=S_{23}^{(2)}(\lambda)=S_{32}^{(2)}(\lambda)=S_{33}^{(2)}(\lambda)=\left[2v_0-\frac{4\alpha^2-7}{4(\alpha^2-1)}\right]g(\lambda)+\frac{\alpha^2}{2(\alpha^2-1)}\frac{\rho_2^4(\lambda)}{\rho_1(\lambda)}, \tag{A.7}$$

where $\alpha=a_1/a$ and

$$g(\lambda)=\begin{cases}-\frac{\alpha^2}{\alpha^2-1}\frac{\rho_2^2(\lambda)}{\rho_1(\lambda)}+\frac{\alpha}{(\alpha^2-1)^{3/2}}\ln\left[(\alpha^2-1)^{1/2}\rho_2(\lambda)+\frac{\alpha\rho_2(\lambda)}{\rho_1(\lambda)}\right] & \text{for } \alpha>1,\\ -\frac{\alpha^2}{\alpha^2-1}\frac{\rho_2^2(\lambda)}{\rho_1(\lambda)}+\frac{\alpha}{(1-\alpha^2)^{3/2}}\tan^{-1}\frac{\alpha}{(1-\alpha^2)^{1/2}\rho_1(\lambda)} & \text{for } \alpha<1.\end{cases} \tag{A.8}$$

Here, λ can be explicitly solved as

$$\lambda=\frac{r^2-a_1^2-a_2^2+\sqrt{(r^2+a_1^2-a_2^2)^2-4(a_1^2-a_2^2)(x_1-x_1^{(1)})^2}}{2}, \tag{A.9}$$

where

$$r^2=(x_i-x_i^{(1)})(x_i-x_i^{(1)}). \tag{A.10}$$

All the other components of the exterior-point Eshelby's tensor can be obtained directly from Eqs. (12)–(16) in Section 2.

In particular, when the inclusion shape becomes spherical ($\alpha=1$), the exterior-point Eshelby's tensor simplifies to

$$\begin{aligned}\bar{G}_{ijkl}(\mathbf{x}-\mathbf{x}_1)=\frac{\rho^3}{30(1-v_0)}\Big[&(3\rho^2+10v_0-5)\delta_{ij}\delta_{kl}+(3\rho^2-10v_0+5)(\delta_{ik}\delta_{jl}+\delta_{il}\delta_{jk})\\&+15(1-\rho^2)\delta_{ij}\hat{n}_k\hat{n}_l+15(1-2v_0-\rho^2)\delta_{kl}\hat{n}_i\hat{n}_j\\&+15(v_0-\rho^2)(\delta_{ik}\hat{n}_j\hat{n}_l+\delta_{il}\hat{n}_j\hat{n}_k+\delta_{jk}\hat{n}_i\hat{n}_l+\delta_{jl}\hat{n}_i\hat{n}_k)+15(7\rho^2-5)\hat{n}_i\hat{n}_j\hat{n}_k\hat{n}_l\Big],\end{aligned} \tag{A.11}$$

where $\rho=a/r$ and a is the radius of the sphere. The above formula is the same as the one given in Ju and Chen (1994c) or Ju and Tseng (1996).

On the contrary, the components of (interior point) Eshelby's tensor of a spheroidal inclusion can be explicitly described as

$$S_{11}^{(1)}(0)=\left[4v_0+\frac{2}{\alpha^2-1}\right]g(0)+4v_0+\frac{4}{3(\alpha^2-1)}, \tag{A.12}$$

$$S_{12}^{(1)}(0)=S_{13}^{(1)}(0)=\left[4v_0-\frac{2\alpha^2+1}{\alpha^2-1}\right]g(0)+4v_0-\frac{2\alpha^2}{\alpha^2-1}, \tag{A.13}$$

$$S_{21}^{(1)}(0)=S_{31}^{(1)}(0)=\left[-2v_0-\frac{1+2\alpha^2}{\alpha^2-1}\right]g(0)-\frac{2\alpha^2}{\alpha^2-1}, \tag{A.14}$$

$$S_{22}^{(1)}(0)=S_{23}^{(1)}(0)=S_{32}^{(1)}(0)=S_{33}^{(1)}(0)=\left[-2v_0+\frac{4\alpha^2-1}{4(\alpha^2-1)}\right]g(0)+\frac{\alpha^2}{2(\alpha^2-1)}, \tag{A.15}$$

$$S_{11}^{(2)}(0)=\left[-4v_0+\frac{4\alpha^2-2}{\alpha^2-1}\right]g(0)-4v_0+\frac{12\alpha^2-8}{3(\alpha^2-1)}, \tag{A.16}$$

$$S_{12}^{(2)}(0) = S_{13}^{(2)}(0) = S_{21}^{(2)}(0) = S_{31}^{(2)}(0) = \left[-v_0 - \frac{\alpha^2+2}{\alpha^2-1} \right] g(0) - 2v_0 - \frac{2}{\alpha^2-1}, \tag{A.17}$$

$$S_{22}^{(2)}(0) = S_{23}^{(2)}(0) = S_{32}^{(2)}(0) = S_{33}^{(2)}(0) = \left[2v_0 - \frac{4\alpha^2-7}{4(\alpha^2-1)} \right] g(0) + \frac{\alpha^2}{2(\alpha^2-1)}, \tag{A.18}$$

where $g(0)$ is given by

$$g(0) = g(\lambda)\,|_{\lambda=0} = \begin{cases} \frac{\alpha}{(\alpha^2-1)^{3/2}} [\cosh^{-1}\alpha - \alpha(\alpha^2-1)^{1/2}] & \text{for } \alpha > 1, \\ \frac{\alpha}{(1-\alpha^2)^{3/2}} [\alpha(1-\alpha^2)^{1/2} - \cos^{-1}\alpha] & \text{for } \alpha < 1. \end{cases} \tag{A.19}$$

For the special case of a spherical inclusion, the (interior point) Eshelby's tensor reduces to

$$S_{ijkl} = \frac{1}{15(1-v_0)} [(5v_0-1)\delta_{ij}\delta_{kl} + (4-5v_0)(\delta_{ik}\delta_{jl} + \delta_{il}\delta_{jk})]. \tag{A.20}$$

Appendix B. An inverse formula for the "generalized isotropic" fourth-rank tensor

Consider the fourth-rank isotropic tensor $\mathbf{Q}$ of the following type:

$$Q_{ijkl} = m\delta_{ij}\delta_{kl} + w(\delta_{ik}\delta_{jl} + \delta_{il}\delta_{jk}), \tag{B.1}$$

where m and w are constants. According to the well-known Sherman–Morrison formula (see, e.g., Dahlquist and Bjorck, 1974), the inverse formula of $\mathbf{Q}$ can be written as

$$Q_{ijkl}^{-1} = -\frac{m}{2w(3m+2w)}\delta_{ij}\delta_{kl} + \frac{1}{4w}(\delta_{ik}\delta_{jl} + \delta_{il}\delta_{jk}). \tag{B.2}$$

Within the proposed framework of micromechanics and homogenization of aligned spheroid-reinforced MMCs, we need to develop the following new "generalized Sherman–Morrison" inversion formula to obtain the inverse tensor of a "generalized isotropic" fourth-rank tensor. That is, we consider a "generalized isotropic" tensor $\mathbf{Q}$ of the form:

$$Q_{ijkl} = (m + M_{IK})\delta_{ij}\delta_{kl} + (w + W_{IJ})(\delta_{ik}\delta_{jl} + \delta_{il}\delta_{jk}), \tag{B.3}$$

where m and w are constants, whereas $\mathbf{M}$ and $\mathbf{W}$ are the second-rank tensors. Moreover, $\mathbf{W}$ should be symmetric. After some derivations, it can be shown that the inverse of $\mathbf{Q}$ in Eq. (B.3) takes the form:

$$Q_{ijkl}^{-1} = -\frac{Y_{IK}}{2(w + W_{II})}\delta_{ij}\delta_{kl} + \frac{1}{4(w + W_{IJ})}(\delta_{ik}\delta_{jl} + \delta_{il}\delta_{jk}), \tag{B.4}$$

where

$$\begin{Bmatrix} Y_{I1} \\ Y_{I2} \\ Y_{I3} \end{Bmatrix} = \begin{bmatrix} m+2w+M_{11}+2W_{11} & m+M_{21} & m+M_{31} \\ m+M_{12} & m+2w+M_{22}+2W_{22} & m+M_{32} \\ m+M_{13} & m+M_{23} & m+2w+M_{33}+2W_{33} \end{bmatrix}^{-1} \begin{Bmatrix} m+M_{I1} \\ m+M_{I2} \\ m+M_{I3} \end{Bmatrix} \tag{B.5}$$

and $I = 1$–3.

The above tensor inversion formula can be easily verified by checking that the product $\mathbf{Q}^{-1} \cdot \mathbf{Q}$ equals the fourth-rank identity tensor $\mathbf{I}$. Specifically, the product $\mathbf{Q}^{-1} \cdot \mathbf{Q}$ leads to

$$Q^{-1}_{ijrs}Q_{rskl} = \left[m + M_{IK} - 2(w + W_{KK})Y_{IK} - \sum_{R=1}^{3}(m + M_{RK})Y_{IR}\right]\frac{\delta_{ij}\delta_{kl}}{2(w + W_{II})} + \frac{1}{2}(\delta_{ik}\delta_{jl} + \delta_{il}\delta_{jk}). \tag{B.6}$$

The coefficient of $\delta_{ij}\delta_{kl}$ term indeed goes to zero.

References

Arsenault, R.J., Fishman, S., Taya, M., 1994. Deformation and fracture behavior of metal-ceramic matrix composite materials. Prog. Mater. Sci. 38, 1–157.

Bao, G., Hutchinson, J.W., McMeeking, R.M.,1991. Particle reinforcement of ductile matrices against plastic flow and creep. Acta Metall. Mater. 39, 1871–1882.

Berveiller, M., Zaoui, A., 1979. An extension of the self-consistent scheme to plastically-flowing polycrystals. J. Mech. Phys. Solids 26, 325–344.

Budiansky, B., Hutchinson, J.W., Slutsky, S., 1982. Void growth and collapse in viscous solids. In: Hopkins, H.G., Sewell, M.J. (Eds.), Mechanics of Solids, The Rodney Hill 60th Anniversary Volume. Pergamon Press, Oxford, pp. 13–45.

Christman, T., Needleman, A., Nutt, S., Suresh, S., 1989a. On microstructural evolution and micromechanical modelling of deformation of a whisker-reinforced metal-matrix composite. Mater. Sci. Engng. A107, 49–61.

Christman, T., Needleman, A., Suresh, S., 1989b. An experimental and numerical study of deformation in metal-ceramic composites. Acta Metall. 37, 3029–3050.

Clyne, T.W., Withers, P.J., 1993. An Introduction to Metal Matrix Composites. Cambridge University Press, MA.

Dahlquist, G., Bjorck, A., 1974. Numerical Methods. Prentice Hall, NJ, p.161.

deBotton, G., Ponte Castaneda, P., 1992. On the ductility of laminated materials. Int. J. Solids Struct. 29, 2329–2353.

Duva, J.M., 1984. A self-consistent analysis of the stiffening effect of rigid inclusions on a power-law material. J. Engng. Mater. Tech. ASME 106, 317–321.

Dvorak, G.J., Bahei-El-Din, Y.A., 1987. A bimodal plasticity theory of fibrous composite materials. Acta Mech. 69, 219–241.

Dvorak, G.J., Bahei-El-Din, Y.A., Macheret, Y., Liu, C.H., 1988. An experimental study of elastic-plastic behavior of a fibrous boron-aluminum composite. J. Mech. Phys. Solids 36, 655–687.

Eshelby, J.D., 1957. The determination of the elastic field of an ellipsoidal inclusion, and related problems. Proc. R. Soc. London. A241, 376–396.

Gurson, A.L., 1977. Continuum theory of ductile rupture by void nucleation and growth. Part I: yield criteria and flow rules for porous ductile media. J. Engng. Mater. Tech. ASME 99, 2–15.

Hansen, A.C., Blackketter, D.M., Walrath, D.E., 1991. An invariant based flow rule for orthotropic plasticity applied to composite materials. J. Appl. Mech. ASME 58, 881–888.

Hashin, Z., 1980. Failure criteria for unidirectional fiber composites. J. Appl. Mech. 47, 329–334.

Hill, R., 1948. A theory of the yielding and plastic flow of anisotropic metals. Proc. R. Soc. London A193, 281–297.

Hom, C.L., 1992. Three-dimensional finite element analysis of plastic deformation in a whisker-reinforced metal matrix composite. J. Mech. Phys. Solids 40, 991–1008.

Ibrahim, I.A., Mohamed, F.A., Lavernia, E.J., 1991. Particulate reinforced metal matrix composites: a review. J. Mater. Sci. 26, 1137–1156.

Ju, J.W., Chen, T.M., 1994a. Micromechanics and effective moduli of elastic composites containing randomly dispersed ellipsoidal inhomogeneities. Acta Mech. 103, 103–121.

Ju, J.W., Chen, T.M., 1994b. Effective elastic moduli of two-phase composites containing randomly dispersed spherical inhomogeneities. Acta Mech. 103, 123–144.

Ju, J.W., Chen, T.M., 1994c. Micromechanics and effective elastoplastic behavior of two-phase metal matrix composites. J. Engng. Mater. Tech. ASME 116, 310–318.

Ju, J.W., Sun, L.Z., 1999. A novel formulation for the exterior-point Eshelby's tensor of an ellipsoidal inclusion. J. Appl. Mech. ASME 66, 570–574.

Ju, J.W., Tseng, K.H., 1996. Effective elastoplastic behavior of two-phase ductile matrix composites: a micromechanical framework. Int. J. Solids Struct. 33, 4267–4291.

Ju, J.W., Tseng, K.H., 1997. Effective elastoplastic algorithms for two-phase ductile matrix composites. J. Engng. Mech. ASCE 123, 260–266.

Kröner, E., 1990. Modified Green function in the theory of heterogeneous and/or anisotropic linearly elastic media. In: Weng, G.J., Taya, M., Abe, H. (Eds.), Micromechanics and Inhomogeneity, The Toshio Mura 65th Anniversary Volume. Springer, New York, pp. 599–622.

Lee, B.J., Mear, M.E., 1991. Effect of inclusion shape on the stiffness of nonlinear two-phase composites. J. Mech. Phys. Solids 39, 627–649.

Lee, B.J., Mear, M.E., 1992. Effective properties of power-law solids containing elliptical inhomogeneities. Part I: rigid inclusions. Mech. Mater. 13, 313–335.

Levy, A., Papazian, J.M., 1990. Tensile properties of short fiber-reinforced SiC/Al composites. Part II: finite-element analysis. Metall. Trans. A 21A, 411–420.

Li, G., 1992. Constitutive Models for Ductile Solids Reinforced by Spheroidal Inclusions, Ph.D. Thesis, Johns Hopkins University, Baltimore, Maryland.

Li,G., Ponte Castaneda, P., 1994. Variational estimates for the elastoplastic response of particle-reinforced metal-matrix composites. Appl. Mech. Rev. ASME 47, S77–S94.

Mazilu, P., 1972. On the theory of linear elasticity in statistically homogeneous media. Rev. Roum. Math. Pures et Appl. 17, 261–273.

Mori, T., Tanaka, K., 1973. Average stress in matrix and average elastic energy of materials with misfitting inclusions. Acta Metall. 21, 571–574.

Mulhern, J.F., Rogers, T.G., Spencer, A.J.M., 1967. A continuum model for a fiber reinforced plastic material. Proc. R. Soc. London. A301, 473–492.

Mura, T., 1987. Micromechanics of Defects in Solids, second edn. Martinus Nijhoff, Boston.

Ponte Castaneda, P., 1991. The effective mechanical properties of nonlinear isotropic composites. J. Mech. Phys. Solids 39, 45–71.

Ponte Castaneda, P., 1992. New variational principles in plasticity and their application to composite materials. J. Mech. Phys. Solids 40, 1757–1788.

Ponte Castaneda, P., 1996. Exact second-order estimates for the effective mechanical properties of nonlinear composite materials. J. Mech. Phys. Solids 44, 827–862.

Qiu, Y.P., Weng, G.J., 1992. A theory of plasticity for porous materials and particle-reinforced composites. J. Appl. Mech. ASME 59, 261–268.

Qiu, Y.P., Weng, G.J., 1993. Plastic potential and yield function of porous materials with aligned and randomly oriented spheroidal voids. Int. J. Plasticity 9, 271–290.

Qiu, Y.P., Weng, G.J., 1995. An energy approach to the plasticity of a two-phase composite containing aligned inclusions. J. Appl. Mech. ASME 62, 1039–1046.

Schmidt, R.J., Wang, D.Q., Hansen, A.C., 1993. Plasticity model of transversely isotropic materials. J. Engng. Mech. ASCE 119, 748–766.

Sun, L.Z., 1998. Micromechanics and Overall Mechanical Behavior of Discontinuously Reinforced Metal Matrix Composites, Ph.D. Thesis, University of California, Los Angeles, California.

Sun, L.Z., Ju, J.W., 2000. Effective elastoplastic behavior of metal matrix composites containing randomly located aligned spheroidal inhomogeneities. Part II: applications. Int. J. Solids Struct. 38, 203–225.

Suquet, P.M., 1993. Overall potentials and extremal surfaces of power law or ideally plastic composites. J. Mech. Phys. Solids 41, 981–1002.

Suresh, S., Mortensen, A., Needleman, A., 1993. Fundamentals of Metal-Matrix Composites. Butterworth-Heinemann, London.

Tandon, G.P., Weng, G.J., 1988. A theory of particle-reinforced plasticity. J. Appl. Mech. ASME 55, 126–135.

Taya, M., Arsenault, R.J., 1989. Metal Matrix Composites: Thermomechanical Behavior. Pergamon Press, Oxford.

Tvergaard, V., 1990. Analysis of tensile properties for a whisker-reinforced metal-matrix composite. Acta Metall. Mater. 38, 185–194.

Voyiadjis, G.Z., Thiagarajan, G., 1995. An anisotropic yield surface model for directionally reinforced metal-matrix composites. Int. J. Plasticity 11, 867–894.

Weng, G.J., 1990. The theoretical connection between Mori-Tanaka's theory and the Hashin-Shtrikman-Walpole bounds. Int. J. Engng. Sci. 28, 1111–1120.

Willis, J.R., 1977. Bounds and self-consistent estimates for the overall properties of anisotropic composites. J. Mech. Phys. Solids 25, 185–202.

Zhao, Y.H., Weng, G.J., 1990. Theory of plasticity for a class of inclusion and fiber-reinforced composites. In: Weng, G.J., Taya, M., Abe, H. (Eds.), Micromechanics and Inhomogeneity, The Toshio Mura 65th Anniversary Volume. Springer, New York, pp. 599–622.

Zhu, H.-T., Zbib, H.M., 1995. A macroscopic model for plastic flow in metal-matrix composites. Int. J. Plasticity 11, 471–499.